


Discovery of a novel dual-targeting D-peptide to block CD24/Siglec-10 and PD-1/PD-L1 interaction and synergize with radiotherapy for cancer immunotherapy

Wenhui Shen,¹ Peishang Shi,² Qingyu Dong,² Xiuman Zhou,¹ Chunxia Chen,² Xinghua Sui,¹ Wentong Tian,² Xueqin Zhu,² Xiaoxi Wang,² Shengzhe Jin,² Yahong Wu,² Guanyu Chen,¹ Lu Qiu,¹ Wenjie Zhai,² Yanfeng Gao ¹

To cite: Shen W, Shi P, Dong Q, *et al.* Discovery of a novel dual-targeting D-peptide to block CD24/Siglec-10 and PD-1/PD-L1 interaction and synergize with radiotherapy for cancer immunotherapy. *Journal for ImmunoTherapy of Cancer* 2023;**11**:e007068. doi:10.1136/jitc-2023-007068

► Additional supplemental material is published online only. To view, please visit the journal online (<http://dx.doi.org/10.1136/jitc-2023-007068>).

Accepted 31 May 2023



© Author(s) (or their employer(s)) 2023. Re-use permitted under CC BY-NC. No commercial re-use. See rights and permissions. Published by BMJ.

¹School of Pharmaceutical Sciences (Shenzhen), Shenzhen Campus of Sun Yat-sen University, Shenzhen, China

²School of Life Sciences, Zhengzhou University, Zhengzhou, China

Correspondence to

Professor Yanfeng Gao; gaoyf29@mail.sysu.edu.cn

Dr Wenjie Zhai; wjzhai@zzu.edu.cn

ABSTRACT

Background Aside from immune checkpoint inhibitors targeting programmed cell death protein 1 (PD-1) and programmed death ligand 1 (PD-L1), intervention of CD47/Sirpα mediated ‘don’t eat me’ signal between macrophage and tumor cell is considered as a promising therapeutic approach for cancer immunotherapy. Compared with CD47, the novel immune checkpoint CD24/Siglec-10 can also deliver ‘don’t eat me’ signal and CD24 shows much lower expression level in normal tissue which might avoid unwanted side effects.

Methods Cell-based phage display biopanning and D-amino acid modification strategy were used to identify the CD24/Siglec-10 blocking peptide. Cell-based blocking assay and microscale thermophoresis assay were used to validate the blocking and binding activities of the peptide. Phagocytosis and co-culture assays were used to explore the in vitro function of the peptide. Flow cytometry was performed to assess the immune microenvironment after the peptide treatment in vivo.

Results A CD24/Siglec-10 blocking peptide (CSBP) with hydrolysis-resistant property was identified. Surprisingly, we found that CSBP could not only block the interaction of CD24/Siglec-10 but also PD-1/PD-L1. CSBP could induce the phagocytosis of tumor cell by both the macrophages and monocytic myeloid-derived suppressor cells (M-MDSCs), which can further activate CD8⁺ T cells. Besides, combination of radiotherapy and CSBP synergistically reduced tumor growth and altered the tumor microenvironment in both anti-PD-1-responsive MC38 and anti-PD-1-resistant 4T1 tumor models.

Conclusions In summary, this is the first CD24/Siglec-10 blocking peptide which blocked PD-1/PD-L1 interaction as well, functioned *via* enhancing the phagocytosis of tumor cells by macrophages and M-MDSCs, and elevating the activity of CD8⁺ T cells for cancer immunotherapy.

INTRODUCTION

In the past few years, there have been significant clinical advances in cancer immunotherapy. The immune checkpoint blockade

WHAT IS ALREADY KNOWN ON THIS TOPIC

- ⇒ Immune checkpoint inhibitors (ICIs) targeting programmed cell death protein 1 (PD-1)/programmed death ligand 1 (PD-L1) have been approved for the treatment of a variety of cancer types. However, only a small subset of patients with cancer can benefit from ICIs.
- ⇒ CD24/Siglec-10 interaction can deliver ‘don’t eat me’ anti-phagocytic signals between macrophages and tumor cells.

WHAT THIS STUDY ADDS

- ⇒ CD24/Siglec-10 blocking peptide (CSBP) is the first reported blocking peptide that can enhance macrophage-mediated phagocytosis of tumor cells and activate CD8⁺ T cells by simultaneously blocking the interaction of CD24/Siglec-10 and PD-1/PD-L1.
- ⇒ We discovered that monocytic myeloid-derived suppressor cells could also mediate phagocytosis effects.
- ⇒ CSBP synergistically inhibits tumor growth combined with radiotherapy in both anti-PD-1-responsive MC38 tumor model and anti-PD-1-resistant 4T1 tumor model.

HOW THIS STUDY MIGHT AFFECT RESEARCH, PRACTICE OR POLICY

- ⇒ CSBP can improve cancer immunotherapy with high therapeutic efficacy by harnessing both innate and adaptive immune responses.

(ICB) strategies have demonstrated unprecedented extension of patient survival, and antibodies targeting programmed cell death protein 1 (PD-1)/programmed death ligand 1 (PD-L1) have been approved to treat various types of cancer, including melanoma and Hodgkin’ lymphoma.¹ However, only a small subset of patients with cancer can benefit

from the immune checkpoint inhibitors (ICIs). The insufficient clinical responses of PD-1/PD-L1 blockade have been reported to be attributed to several reasons, such as low-expression of PD-L1, low immune cell infiltration, low tumor mutation burden and so on.² Therefore, it is urgent to discover novel drug targets for developing therapeutic agents and combination strategies to enhance the response rate of cancer immunotherapy.

Different from the blockade of PD-1/PD-L1 to initiate antitumor immune response through CD8⁺ T cells, interference of the 'don't eat me' pathway mediated by macrophages has many advantages.³ First, the distribution of macrophage is more common in most solid tumors than CD8⁺ T cell. Second, the antigen from the phagocytosed tumor cell can be subsequently processed and presented to T cell by macrophages, which can also function as antigen-presenting cells.⁴ Therefore, several involving pathways have been reported and considered as therapeutic targets, especially CD47/Sirp α . Antibodies and fusion proteins targeting CD47 were developed and studied clinically.⁵ Unfortunately, because of the wide expression of CD47 in normal tissues as well, side effects and low therapeutic efficacy often arise mainly caused by non-tumor-targeting.⁶ Due to the relatively weak receptor occupation and promising tumor penetration properties of small peptides compared with antibodies, thus we have developed a small peptide to block CD47/Sirp α previously, which could elicit antitumor effects alone or combined with radiotherapy (RT) without significant toxicity.⁷ Therefore, it is a promising strategy to develop small peptides as therapeutic agents targeting immune checkpoints.

Recently, another 'don't eat me' pathway, CD24/Siglec-10, has been revealed.⁸ CD24 is a mucin-like glycosylphosphatidylinositol-anchored glycoprotein, which is expressed in murine hematopoietic cell subpopulations, including B lymphocytes,⁹ the majority of thymocytes,¹⁰ erythrocytes and neutrophils.¹¹⁻¹² CD24 is responsible for proliferation of T lymphocytes as a co-stimulatory molecule, as it is crucial for the homeostatic proliferation of T cells in the lymphopenic environment.¹³ More importantly, compared with CD47, CD24 is absent on human erythrocytes or thymocytes but highly expressed in various cancer cells and cancer stem cells.⁸ CD24 has been identified as a prognostic marker in patients with ovarian cancer,¹⁴ lung cancer,¹⁵ and it is also involved in the migration and metastasis of glioblastoma cells and osteosarcoma cells.¹⁶⁻¹⁷ Therefore, CD24 has recently attracted much attention as a potential drug target against cancer cells or cancer stem cells.

CD24 interacted with Siglec-10, relaying anti-phagocytic signals to cause tumor cells to evade immune killing. Accordingly, anti-CD24 could induce macrophage-mediated phagocytosis of ovarian cancer and breast cancer cells and reduce tumor burden in MCF-7 tumor model.⁸ The expression of CD24 is higher than PD-L1 in several cancers, including which resistant to anti-PD-1 therapy.⁸ As CD24 is overexpressed in tumor tissues whereas rarely

detected in normal tissues, it is necessary to further determine the potential and develop therapeutic agents to block CD24/Siglec-10 for cancer immunotherapy.

The anti-CD24 monoclonal antibody (mAb) SWA11 effectively inhibited tumor cell proliferation and angiogenesis with retarding ovarian carcinoma xenografts growth.¹⁸ In CD24-positive triple negative breast cancer (TNBC), CD24 mAb (ALB9) treatment significantly reduced lung tumor growth and greatly prolonged the survival of mice.¹⁹ Compared with proteins and antibodies, small peptides are less immunogenic and have better tumor permeability. Peptides are generally low-cost and easy to synthesize. On the other hand, compared with small molecules, peptides are usually characterized by lower toxicity, higher efficacy and specificity.²⁰ In the previous studies, we have identified small peptides as ICIs targeting PD-1/PD-L1, lymphocyte activation gene 3 (LAG-3)/major histocompatibility complex (MHC)-II, T cell immunoreceptor with Ig and ITIM domains (TIGIT)/poliovirus receptor (PVR) and CD47/Sirp α , respectively.^{7 21-23} However, the development of peptide drugs targeting the 'don't eat me' signal CD24/Siglec-10 has not been reported yet.

Here, the CD24 and CD47 expression was analyzed and compared, and the phage display peptide library biopanning technology was used to screen CD24 binding peptides. Retro-inversion and glutamic acid substitution strategies were performed to improve the hydrolysis-resist ability and solubility, respectively. By using a cell-based blocking assay, an 8-mer CD24/Siglec-10 blocking peptide (CSBP) composed of D-amino acids was identified. Surprisingly, CSBP could also block the interaction of PD-1/PD-L1, which resulted in promoting the phagocytosis of macrophages and activating CD8⁺ T cells. We also investigated whether CSBP could enhance the phagocytosis of monocytic myeloid-derived suppressor cell (M-MDSC). Finally, the antitumor response of CSBP alone or combined with RT was studied. Thus, this study proposed new insights and strategies to harness both myeloid cells and T cells for cancer immunotherapy, by using small peptides as dual-targeting ICIs combined with RT.

MATERIALS AND METHODS

Cell lines

MDA-MB-231, HT29, 4T1 and CT26 cells were grown in RPMI-1640 medium, and MDA-MB-453, MDA-MB-468 and MC38 cells were cultured in DMEM. The medium contained 10% fetal bovine serum (Gibco, Grand Island, New York, USA), 1% penicillin/streptomycin solution.

Mouse tumor models

For MC38 model, 1×10^6 MC38 cells were subcutaneously injected into the right flank of 35 female SPF-level C57BL/6 mice (6-week-old) randomly divided into seven groups to develop the subcutaneous tumor bearing model. The sample size was determined according to the

previous research results of our group and others. For CSBP treatment, 2 mg/kg of CSBP was daily injected intraperitoneally (*i.p.*) into the mice. For antibodies, 400 µg of anti-mouse CD47 antibody (miap301, Bio X Cell, USA), 250 µg of anti-PD-L1 (10F.9G2, Bio X Cell, USA), 200 µg of anti-CD24 (M1/69, Bio X Cell, USA), or 250 µg of anti-PD-L1 plus 200 µg of anti-CD24, were injected *i.p.* into the mice every 3 days. Phosphate buffered saline containing 5% DMSO and rat IgG were used as the negative controls, respectively. Tumor volumes were measured every other day by length (a), width (b) and height (c), and calculated as tumor volume=abc/2. Treatment was continued for 2 weeks, then the mice were euthanized, tumors, spleens and draining lymph nodes were dissected. For macrophages depletion, 150 µL of clodronate liposomes or control liposomes (FormuMax Scientific, USA) were injected *i.p.* into C57BL/6 mice. The efficiency of macrophages depletion was tested by analyzing the CD45⁺ CD11b⁺ F4/80⁺ cells. For M-MDSCs depletion, 100 µg of anti-mouse Gr-1 (RB6-8C5, Bio X Cell, USA) was delivered by *i.p.* injection every 3 days with rat IgG as the negative controls. The efficiency of M-MDSCs depletion was tested by analysis of the CD45⁺ CD11b⁺ Ly6G⁻ Ly6C⁺ cells. In the MC38 RT model, tumor-bearing mice were treated with local 20 Gy RT, and CSBP (2 mg/kg) was administered *i.p.* to mice daily.

For the 4T1 model, 5 × 10⁴ 4T1 cells were inoculated orthotopically in the BALB/c mice mammary fat pad. In the 4T1 RT model, tumor-bearing mice were treated 12 Gy RT twice and treated with CSBP (2 mg/kg) daily.

Statistical analysis

Differences between groups were analyzed by unpaired Student's t-test or two-way analysis of variance. All data are presented as means ± SEM. Statistical analyses were carried out using Prism V.8.0 statistical software (GraphPad Software). Flow cytometry data were analyzed by FlowJo V.10. Significant differences between the groups are indicated by *p < 0.05, **p < 0.01, ***p < 0.001.

RESULTS

CD24 is overexpressed in tumor tissues and associated with poor prognosis

The CD24 expression was assessed in tumor and normal tissues *via* analyzing the UALCAN data portal, which revealed that CD24 was overexpressed in several cancer types, such as kidney renal papillary cell carcinoma, esophageal carcinoma, and breast invasive carcinoma (BRCA) (figure 1A). The high expression of CD24 was associated with poor prognosis in BRCA (p = 0.00021), mesothelioma (p = 0.0034), cervical squamous cell carcinoma and endocervical adenocarcinoma (p = 0.045) using gene expression profiling interactive analysis (GEPIA) (figure 1B). Interestingly, the expression of CD24 differed in BRCA subtypes, and it was significantly higher in TNBC basal-like 1 than that in normal breast, luminal or HER2⁺ BRCA (figure 1C). The expression level of CD24 was

much higher than that of PD-L1 in most BRCA subtypes (figure 1C). In addition, single-cell RNA-sequencing data demonstrated that CD24 was expressed higher than PD-L1 in both T-cell expansion and T-cell non-expansion groups after anti-PD-1 treatment (figure 1D).²⁴ The CD24 and PD-L1 expression on various tumor cell lines were displayed (figure 1E). CD24 and CD47 expression were highly expressed in multiple tumor types by analyzing GEPIA (online supplemental figure S1A). Meanwhile, the BioGPS database results suggested that the expression of CD47 was significantly higher than that of CD24 expression in most of the normal tissues, such as skin, liver, pituitary, lung and heart (online supplemental figure S1B). These results illustrated the advantages of CD24 as a potential drug target for immunotherapy.

Screening of candidate peptides binding CD24 via a cell-based phage display biopanning

To obtain CD24-binding peptides, a random 7-mer peptide library was used for the cell-based phage display biopanning. High-affinity phages were productively enriched after four rounds of screening. We isolated and sequenced the DNA of the phage clones, then the sequences of corresponding peptides were aligned *via* Clustal Omega. Finally, peptides with different common sequences were selected, and their sequences were displayed in online supplemental table S1. The blocking activity of candidate peptides for CD24/Siglec-10 interaction was verified by the blocking assay. As shown in online supplemental table S1, the blocking rates of peptide-9, peptide-6 and peptide-5 were 55.70%, 39.03% and 18.43%, respectively. Therefore, peptide-9 with the highest blocking rate was selected as the candidate peptide. Alanine scanning of peptide-9 was performed to help further rationalized modifications.²⁵ The results confirmed that each amino acid was essential for blocking CD24/Siglec-10 interaction, with L3, F4 and V5 were the key residues to interact with CD24 (online supplemental table S2). Peptide-9 was named blocking peptide (BP) for further investigation.

CSBP binds CD24 and PD-L1, targeting CD24/Siglec-10 and PD-1/PD-L1 pathways

L-amino acids were sensitive to proteases and could be degraded easily.²⁶ To improve the hydrolysis stability of BP, we attempted to transform some L-amino acids into D-configuration amino acids.²⁷ According to the alanine scanning results, L-amino acids were substituted with D-amino acids except for L3, F4 and V5, and the retro-inverso peptide harboring the reverse sequence of BP was also designed. As shown in figure 2A, the retro-inverso peptide (^DBP-1) was able to block the interaction of CD24/Siglec-10, but the decreased blocking ability was observed in BP-2 and BP-3. To increase the solubility of ^DBP-1, C-terminal and N-terminal residues were modified by the hydrophilic glutamic acid.²⁸ We found that C1e (CSBP) exhibited greater blocking activity than ^DBP-1 (figure 2A). CSBP exhibited dose-dependent effect to block human CD24/Siglec-10 interaction with a good

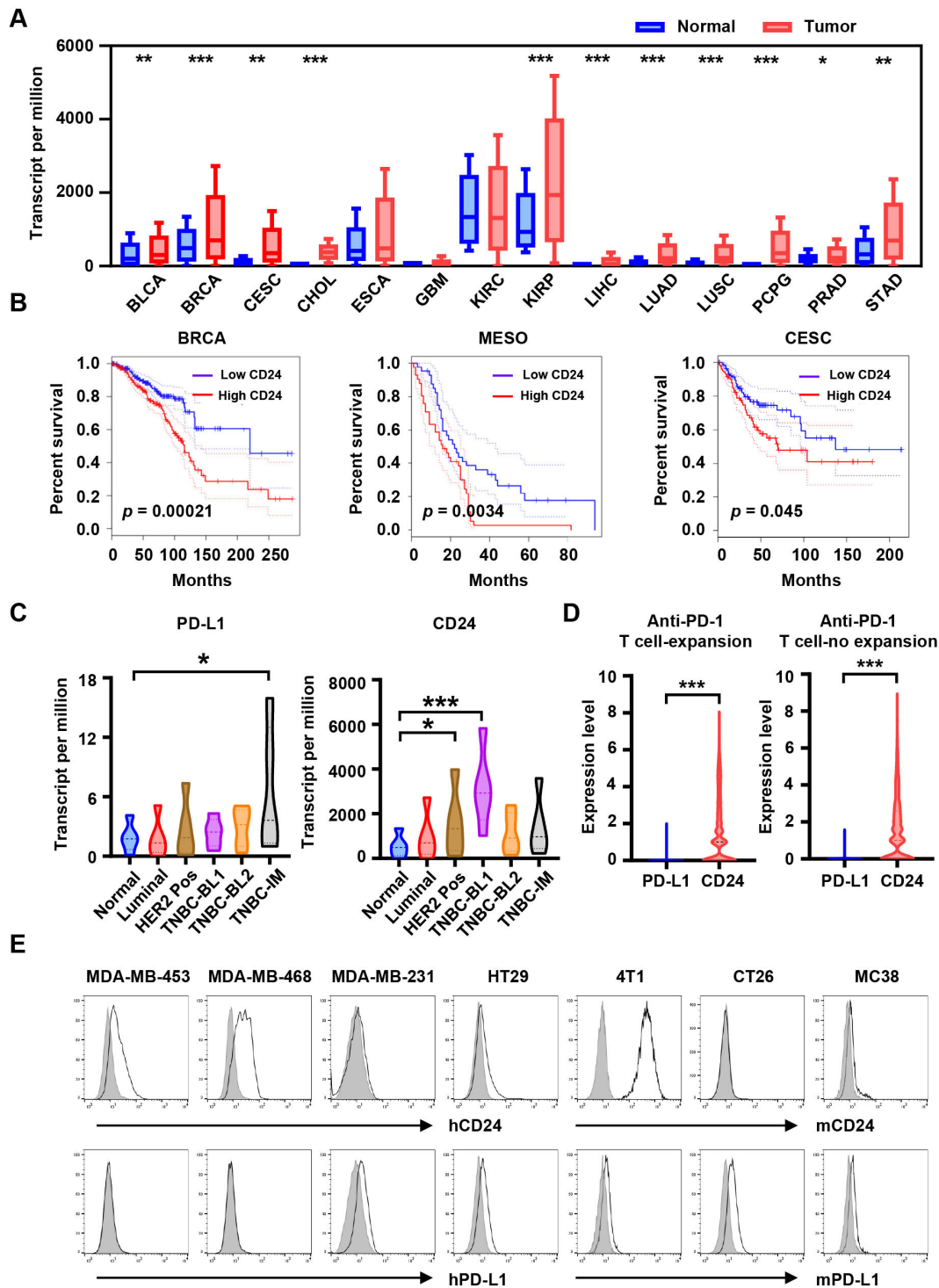


Figure 1 CD24 is significantly overexpressed in tumors. (A) Expression of CD24 across multiple human cancers (red) compared with corresponding normal tissues (blue) obtained from the UALCAN database. (B) The overall survival curve of human cancers with high and low CD24 expression analyzed by the GEPIA. (C) Expression of PD-L1 and CD24 in BRCA major subclasses *via* UALCAN database. (D) Expression analysis of PD-L1 and CD24 in human TNBC cells from patients (n=5) where T expansion or no-expansion to anti-PD-1 immunotherapy across single cell sequencing illustrated. (E) Expression of CD24 and PD-L1 on human or mouse tumor cell lines was detected by flow cytometry, gray shading indicates matched isotype controls. Data are presented as means \pm SEM, and statistical significance was determined by unpaired Student's t-test. *p<0.05, **p<0.01, ***p<0.001. BLCA, bladder Urothelial Carcinoma; BRCA, breast invasive carcinoma; CESC, cervical squamous cell carcinoma and endocervical adenocarcinoma; CHOL, cholangiocarcinoma; ESCA, esophageal carcinoma; GBM, glioblastoma multiforme; GEPIA, gene expression profiling interactive analysis; KIRC, kidney renal clear cell carcinoma; KIRP, kidney renal papillary cell carcinoma; LIHC, liver hepatocellular carcinoma; LUAD, lung adenocarcinoma; LUSC, lung squamous cell carcinoma; MESO, mesothelioma; PCPG, pheochromocytoma and paraganglioma; PD-1, programmed cell death protein 1; PD-L1, programmed death ligand 1; PRAD, prostate adenocarcinoma; STAD, stomach adenocarcinoma; TNBC, triple negative breast cancer.

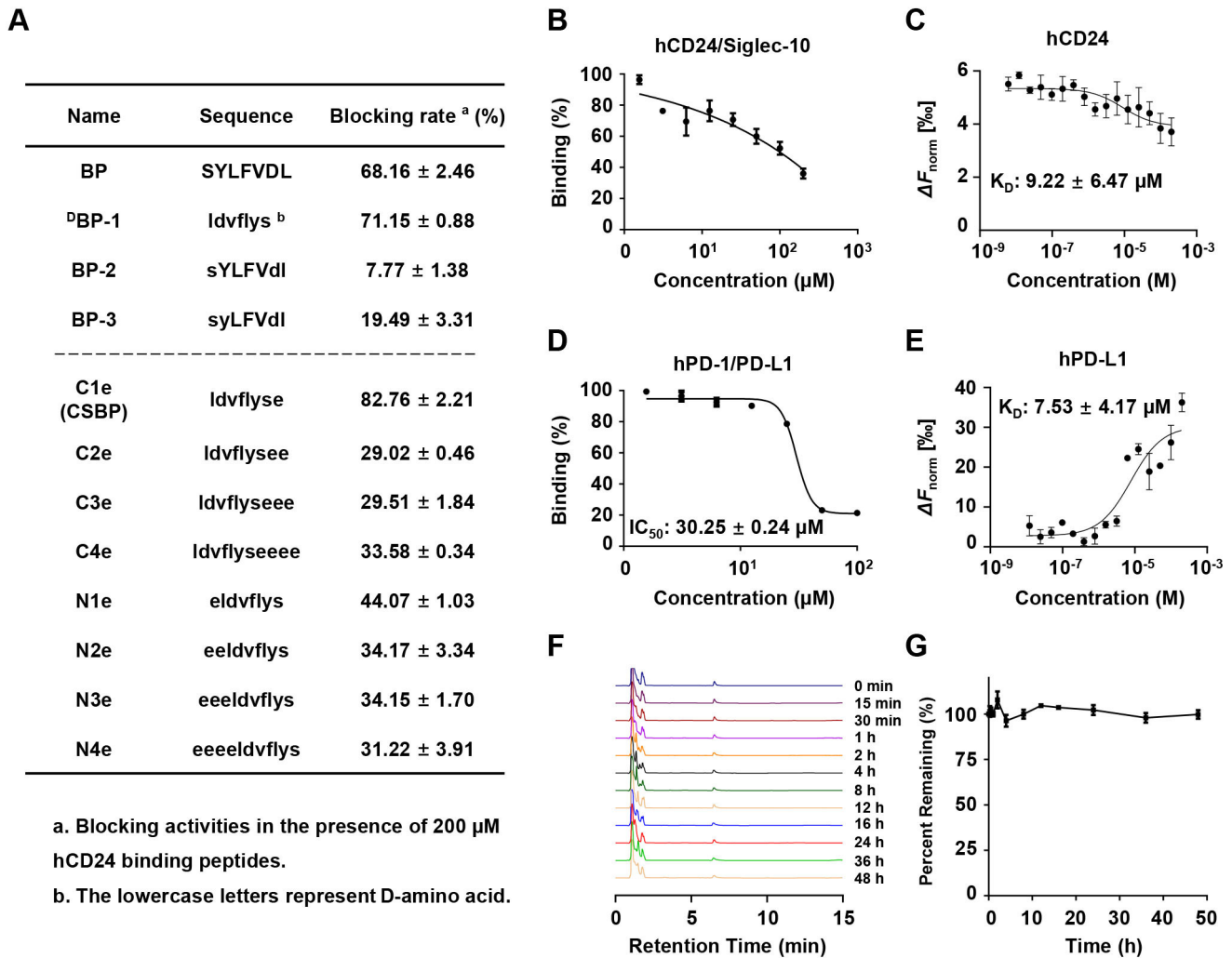


Figure 2 Characterization of bispecific peptide targeting CD24/PD-L1. (A) Blocking activities of optimized peptides. (B) In vitro blocking activity of CSBP on the human CD24/hSiglec-10 interaction as measured by flow cytometry. (C) In vitro binding affinity of CSBP on human CD24 as measured by MST. (D) In vitro blocking activity of CSBP on the human PD-1/PD-L1 interaction as measured by flow cytometry. (E) Binding affinity of CSBP on human PD-L1 as measured by MST. (F) Representative HPLC analysis of CSBP hydrolysis in 10% human serum. (G) The residual peptide time-dependent curve. Data are presented as means±SEM. BP, blocking peptide; CSBP, CD24/Siglec-10 blocking peptide; HPLC, high performance liquid chromatography; MST, microscale thermophoresis; PD-1, programmed cell death protein 1; PD-L1, programmed death ligand 1.

affinity to human CD24 ($K_D=9.22\pm 6.47\mu\text{M}$) (figure 2B,C). Interestingly, we found that CSBP also blocked the human PD-1/PD-L1 interaction ($IC_{50}=30.25\pm 0.24\mu\text{M}$) (figure 2D). Additionally, CSBP illustrated good affinity to human PD-L1 ($K_D=7.53\pm 4.17\mu\text{M}$) (figure 2E). Due to the lack of commercial availability of mouse Siglec-10 protein, we attempted to test whether human Siglec-10 could bind to 4T1 cells overexpressing murine CD24. The results demonstrated that human Siglec-10 could bind to 4T1 cells overexpressing murine CD24. The high similarity between human Siglec-10 and mouse Siglec-10 with an overall homology of about 60% can explain this phenomenon. Peptide CSBP demonstrated relative high blocking effect on mCD24/hSiglec-10 interaction (online supplemental figure S2A), and exhibited an affinity to mCD24 ($K_D=0.22\pm 0.18\mu\text{M}$) (online supplemental figure S2B). The blockade of CSBP to mouse PD-1/PD-L1 interaction was determined ($IC_{50}=55.64\pm 0.14\mu\text{M}$),

and the affinity with mouse PD-L1 was determined ($K_D=22.9\pm 14.7\mu\text{M}$) (online supplemental figure S2C,D). To verify the stability of CSBP, the kinetics of degradation were monitored by reverse phase-high performance liquid chromatography (RP-HPLC). CSBP exhibited resistance to protease degradation in 10% human serum or mouse serum (figure 2F,G; online supplemental figure S2E,F). These results suggested that peptide CSBP could block CD24/Siglec-10 and PD-1/PD-L1 interactions and was hydrolysis-resistant in the serum.

To explore whether CSBP could target the CD24/Siglec-10 and PD-1/PD-L1 interactions, we measured the blocking activity of CSBP on other immune checkpoints, including CD47/Sirp α , TIGIT/PVR, LAG-3/FGL1 and LAG-3/MHC-II. The results showed that CSBP did not exert blocking activity in these targets (online supplemental figure S3A). In addition, among other peptides blocking CD24/Siglec-10 interaction,

N2e could also simultaneously block the PD-1/PD-L1 interaction (online supplemental figure S3B). While the previously discovered PD-1/PD-L1 targeting peptide OPBP-1 and the CD47/Sirp α targeting peptide pep-20 were unable to block CD24/Siglec-10 (online supplemental figure S3C).^{7,29} In order to study the mechanism of CSBP targeting CD24/Siglec-10 and PD-1/PD-L1, the ESPrpt was used to generate sequence alignment. The results indicated that the sequences of the Siglec-10 IgV domain were partly consistent with PD-1, among which Leu128, Ala132, Ile134 and Glu136 were the key residues to interact with PD-L1 (online supplemental figure S3D). We next predicted Siglec-10 and CSBP structure by PEP-FOLD3. Three-dimensional structural prediction and molecular docking analysis (MOE) were used to compare structural similarity between PD-1 (PDB: 4ZQK) and Siglec-10 protein (online supplemental figure S3E). The key residues and binding regions of CSBP and PD-L1 protein were simulated by the MOE. CSBP might interact with PD-L1 (PDB: 5C3T) through Asp2-Arg113, Val3-Glu58, Glu8-Gln66, among which Arg113, Glu58 and Gln66 were the key residues to interact with PD-1 (online supplemental figure S3F). The interaction residues of CSBP and CD24 were not analyzed due to the lack of crystal structure of CD24 and CD24/Siglec-10 interface. These results suggested that CSBP may target CD24/Siglec-10 and PD-1/PD-L1 because of the similarity of the amino acid sequence and protein structure between PD-1 and Siglec-10 protein.

CSBP enhances macrophage-mediated and M-MDSC-mediated phagocytosis of tumor cells and potentiates the function of CD8⁺ T cells in vitro

Human Siglec-10 has been reported to be expressed on tumor-associated macrophages (TAMs). We observed the expression of mouse Siglec-G (homologue of human Siglec-10 in murine) in TAMs, the M-MDSC and granulocytic myeloid-derived suppressor cells (G-MDSC) (figure 3A). Then, we investigated whether CSBP could enhance the phagocytosis of CD24⁺ tumor cells. CSBP showed no cytotoxic effects on 4T1 and MC38 cells by 3-(4,5-dimethylthiazol-2-yl)-2,5-diphenyltetrazolium bromide (MTT) (online supplemental figure S4A). Incubation of 4T1 and MC38 cells with CSBP or anti-CD47 antibody (positive control) treatment resulted in significant phagocytosis by bone marrow-derived macrophages (BMDM) (figure 3B; online supplemental figure S4B). The splenocytes of 4T1 tumor-bearing mice were co-cultured with 4T1 labeled with carboxyfluorescein succinimidyl ester (CFSE) for 2 hours to detect macrophage and M-MDSC-mediated phagocytosis. Amazingly, we found the phagocytosis of 4T1 cells exhibited a significant increase not only to macrophage but also to M-MDSC, after treatment of CSBP or anti-CD47 antibody (figure 3C,D). To explore whether CD8⁺ T cells can be primed after CSBP-mediated phagocytosis by macrophages, we examined the percentage of proliferating CD8⁺ T cells via CFSE assay. BMDM were co-cultured with 4T1 cells in the presence of

CSBP. The percentage of proliferating CD8⁺ T cells and the ratio of interferon (IFN)- γ -expressing T cells were significantly increased, which indicated that it could activate CD8⁺ T-cell immune activity following macrophage-mediated phagocytosis by CSBP (online supplemental figure 5A,B).

To prove the effect of CSBP blocking the PD-1/PD-L1 pathway, Jurkat cells were used as a model T-cell line. When Jurkat cells were co-cultured with PD-L1 overexpressed CHO-K1-hPD-L1 cells, the proportion of interleukin (IL)-2⁺ CD45⁺ T cells decreased from 9.61% to 4.08%. The proportion of IL-2⁺ CD45⁺ T cells restored to 8.4% after CSBP treatment (figure 3E). Relative to co-cultured with CHO-K1-Vec cells which did not express PD-L1, the proportion of IL-2⁺ CD45⁺ T cells was unaffected in the presence or absence of CSBP. To further determine this promotion effect induced by CSBP depended on the blocking of PD-1/PD-L1, human peripheral blood mononuclear cells (PBMCs) were co-cultured with PD-L1 overexpressed CHO-K1-hPD-L1 for 3 days. The results indicated that PD-1/PD-L1 interaction directly inhibited the proliferation of CD8⁺ T cells and reduced the proportion of IFN- γ -expressing CD8⁺ T cells, which were restored by CSBP treatment (figure 3F,G). When PBMCs were co-cultured with CHO-K1-Vec cells which did not express PD-L1, the proliferation of CD8⁺ T cells and proportion of IFN- γ -expressing CD8⁺ T cells were not affected with or without CSBP, which were consistent with the results from Jurkat cells co-culture assay. Based on the results, it can be concluded that CSBP abrogated the PD-1/PD-L1 axis-mediated dysfunction of T cells, further suggesting that CSBP could regulate T-cell function by blocking PD-1/PD-L1 interaction. In conclusion, CSBP could activate CD8⁺ T cells both indirectly through macrophage-mediated phagocytosis and directly by blocking PD-1/PD-L1 interaction.

CSBP inhibits tumor growth in MC38 model

MC38 tumor model was performed to test the responses of cytotoxic T cells against cancer cells, including PD-1/PD-L1 blockade. We first explored the antitumor response of CSBP in this model. Besides, we evaluated the antitumor response of CSBP with other groups, including anti-PD-L1, anti-CD24, and anti-PD-L1 plus anti-CD24. Although anti-PD-L1 and anti-CD24 significantly inhibited tumor growth, the tumor volume was bigger than the treatment with CSBP. Moreover, the antitumor response of CSBP was similar to that of anti-PD-L1 plus anti-CD24 treatment (figure 4A,B). Compared with anti-CD24 or anti-PD-L1 monotherapy, the CSBP treatment group significantly enhanced the percentage of tumor-infiltrating T cells (figure 4C). Also, CSBP simultaneously enhanced the cytotoxic activity of T cells. The percentage of IFN- γ -expressing CD8⁺ T cells was increased with CSBP treatment, compared with anti-PD-L1 or anti-CD24 monotherapy (figure 4D). In addition to T cells, CSBP increased the ratio of M1/M2 (figure 4E). Furthermore, the CSBP treatment group increased the frequency of M-MDSCs.

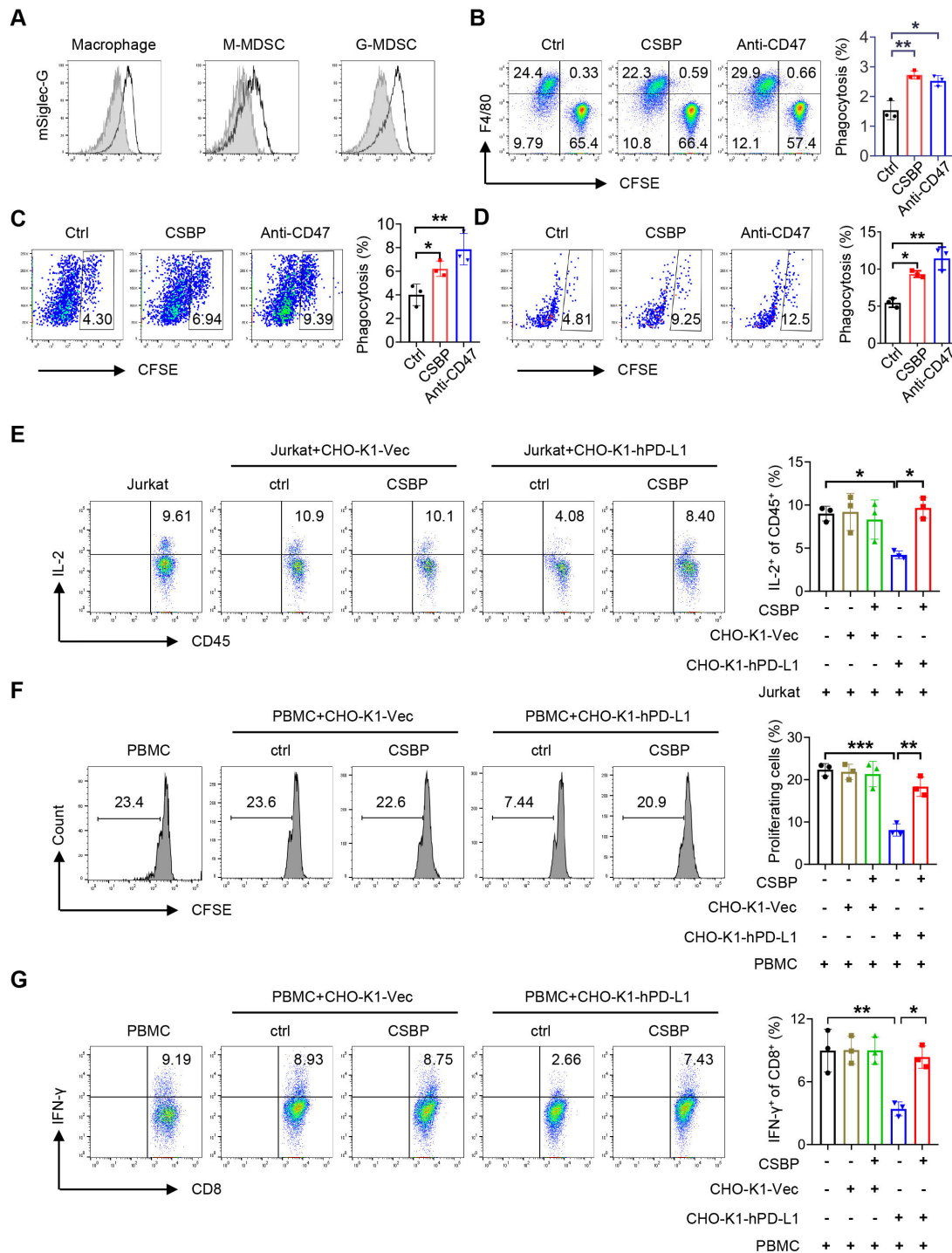


Figure 3 4T1 cancer cells phagocytosis by macrophage/M-MDSC and T-cell activation after CSBP treatment. (A) Representative flow cytometry histogram of the expression of mSiglec-G (black lines) versus isotype control (gray shaded curves) by macrophage, M-MDSC or G-MDSC. (B) Phagocytosis assays were performed with CD24⁺ 4T1 cells by BMDMs in the presence of CSBP or anti-CD47 mAb. (C, D) Flow cytometry analysis of phagocytosis of 4T1 cells by macrophages and M-MDSCs from 4T1 tumor-bearing mice spleen, in the presence of CSBP or anti-CD47 mAb. (E) Evaluation of the effects of CSBP on IL-2-expressing Jurkat T cells. Intracellular staining of IL-2 was detected by flow cytometry. (F, G) PBMCs from healthy donors were isolated and stained with 0.2 μM CFSE. Then, PBMCs were activated with 100 U/mL IL-2, 1 μg/mL anti-CD3, and 1 μg/mL anti-CD28 stimulatory antibodies, and cultured with CHO-K1-Vec or CHO-K1-hPD-L1 cells with or without CSBP. After 3 days, the proliferation of CD8⁺ T cells and proportion of IFN-γ-expressing CD8⁺ T cells were analyzed by flow cytometry. Data are representative of at least three independent experiments. Data are presented as means ± SEM, and statistical significance was determined by two-way analysis of variance with multiple comparisons. *p < 0.05, **p < 0.01, ***p < 0.001. BMDMs, bone marrow-derived macrophages; CFSE, carboxyfluorescein succinimidyl ester; CSBP, CD24/Siglec-10 blocking peptide; G-MDSC, granulocytic myeloid-derived suppressor cell; IFN, interferon; IL, interleukin; mAb, monoclonal antibody; M-MDSC, monocytic myeloid-derived suppressor cell; PBMCs, peripheral blood mononuclear cells.

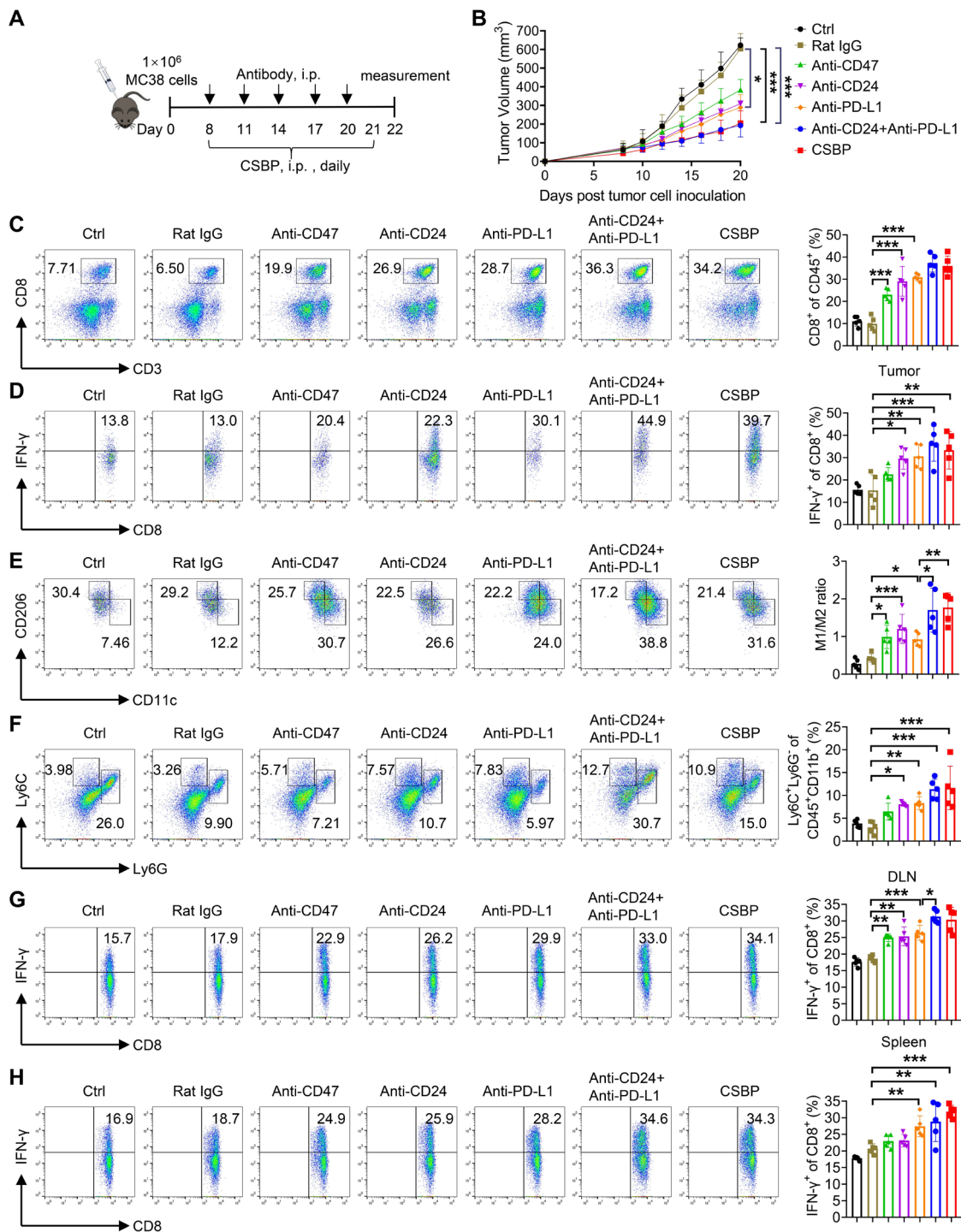


Figure 4 CSBP inhibits tumor growth in MC38 tumor model. (A) Schematic of the dosing schedule time points for treatment groups. (B) The tumor growth curves of MC38-bearing mice receiving the treatment of CSBP or antibodies. Data are presented as the means ± SEM (n=5 per group). (C) The percentage of tumor-infiltrating CD8⁺ T cells in total CD45⁺ cells was determined by flow cytometry (n=5). (D) The frequency of IFN-γ-expressing CD8⁺ T cells was detected by flow cytometry (n=5). (E) Flow cytometric analysis of M1/M2 ratio in the TME after CSBP or antibodies treatment (n=5). M1, CD45⁺ CD11b⁺ F4/80⁺ CD11c⁺ CD206⁻; M2, CD45⁺ CD11b⁺ F4/80⁺ CD206⁺ CD11c⁻. (F) Percentages of myeloid-derived suppressor cell within the TME in each group (n=5). G-MDSC, CD45⁺ CD11b⁺ Ly6G⁺ Ly6C⁻; M-MDSC, CD45⁺ CD11b⁺ Ly6G⁻ Ly6C⁺. (G, H) Cells from mice draining lymph nodes (G) or spleens (H) were obtained and stimulated with 20 ng/mL of PMA and 1 μM ionomycin containing protein transport inhibitor cocktail for 4 hours. Frequencies of IFN-γ-expressing CD8⁺ T cells were detected by flow cytometry (n=5). Data are presented as means ± SEM, and statistical significance was determined by two-way analysis of variance with multiple comparisons. *p<0.05, **p<0.01, ***p<0.001. CSBP, CD24/Siglec-10 blocking peptide; G-MDSC, granulocytic myeloid-derived suppressor cell; IFN, interferon; i.p., intraperitoneally; M-MDSC, monocytic myeloid-derived suppressor cell; PD-L1, programmed death ligand 1; PMA, phorbol 12-myristate 13-acetate; TME, tumor microenvironment.

The frequency of M-MDSCs in the CSBP-treated group showed higher than that in other groups (figure 4F). In addition, the CSBP treatment group showed an increased percentage of IFN- γ -expressing CD8⁺ T cells in draining lymph nodes and spleens, compared with treatment of anti-PD-L1 or anti-CD24 (figure 4G,H).

The antitumor effect of CSBP is partially dependent on macrophages

To investigate the importance of macrophages in anti-tumor response, clodronate liposomes were used to deplete macrophages in MC38 tumor-bearing mice. In comparison with control liposome, macrophages have shown to be effectively removed from the peripheral blood with clodronate liposome (online supplemental figure S6). The schedule of administration of clodronate liposome or control liposome was shown in online supplemental figure S7A. Depletion of macrophages partially abolished the antitumor effect by CSBP treatment ($p < 0.001$, ctrl plus control liposome vs CSBP plus control liposome; $p = 0.086$, ctrl plus clodronate liposome vs CSBP plus clodronate liposome) (online supplemental figure S7B). When macrophages were depleted, the increase of the percentage of tumor infiltrated CD8⁺ T cells was not significantly changed after CSBP treatment ($p < 0.001$, ctrl plus control liposome vs CSBP plus control liposome; $p = 0.0027$, ctrl plus clodronate liposome vs CSBP plus clodronate liposome), and the increase of the percentage of tumor infiltrated IFN- γ -expressing CD8⁺ T cells ratio exhibited slight decrease ($p = 0.1148$, ctrl plus control liposome vs CSBP plus control liposome; $p = 0.4135$, ctrl plus clodronate liposome vs CSBP plus clodronate liposome) (online supplemental figure S7C,D). Furthermore, when macrophages were depleted, the ratio of M-MDSCs was not significantly affected with CSBP treatment ($p = 0.1059$, ctrl plus control liposome vs CSBP plus control liposome; $p = 0.8744$, ctrl plus clodronate liposome vs CSBP plus clodronate liposome) (online supplemental figure S7E). When macrophages were depleted, the increase of IFN- γ -expressing CD8⁺ T cells with CSBP treatment in draining lymph nodes and spleens was slightly impaired, especially in the lymph nodes (online supplemental figure S7F,G). The data suggested that the antitumor effect of CSBP was partially dependent on macrophages.

M-MDSCs play an important role in the antitumor effect of CSBP

To further delineate the role of M-MDSC in the anti-tumor effects of CSBP, myeloid-derived suppressor cell (MDSC) depletion experiments were performed in MC38 tumor model using the anti-Ly6G/Ly6C (Gr-1) antibody. When C57BL/6 mice were treated with the anti-Ly6G/Ly6C (Gr-1) antibody, there was an efficient depletion of G-MDSCs and M-MDSCs compared with the control IgG (online supplemental figure S8). The schedule of dosing was shown in online supplemental figure S9A. Depletion of M-MDSCs significantly attenuated the anti-tumor effect of CSBP, but the statistical difference did

not change ($p < 0.0001$, ctrl plus rat IgG vs CSBP plus rat IgG; $p < 0.0001$, ctrl plus anti-Gr-1 vs CSBP plus anti-Gr-1) (online supplemental figure S9B). When M-MDSCs were depleted, the increase of the percentage of tumor infiltrated CD8⁺ T cells was slightly impaired ($p = 0.0115$, ctrl plus rat IgG vs CSBP plus rat IgG; $p = 0.6287$, ctrl plus anti-Gr-1 vs CSBP plus anti-Gr-1), and the ratio of IFN- γ -expressing CD8⁺ T cells was not significantly changed after CSBP treatment ($p = 0.0103$, ctrl plus rat IgG vs CSBP plus rat IgG; $p = 0.0401$, ctrl plus anti-Gr-1 vs CSBP plus anti-Gr-1) (online supplemental figure S9C,D). Furthermore, the ratio of M1/M2 was slightly increased with CSBP treatment after M-MDSCs were depleted ($p = 0.0855$, ctrl plus rat IgG vs CSBP plus rat IgG; $p = 0.9113$, ctrl plus anti-Gr-1 vs CSBP plus anti-Gr-1) (online supplemental figure S9E). When M-MDSCs were depleted, the percentage of IFN- γ -expressing CD8⁺ T cells was increased after CSBP treatment in spleens but not in draining lymph nodes (online supplemental figure S9F,G). The data showed that M-MDSCs played an important role in the antitumor effect of CSBP.

CSBP combined with radiotherapy exerts synergistically antitumor effect in MC38 tumor model

We verified that CSBP targeting PD-1/PD-L1 showed excellent antitumor effect. In addition, RT can recruit tumor immune cells and upregulate PD-L1 expression.³⁰ To investigate the therapeutic potential of CSBP combined with local RT, C57BL/6 mice with MC38 tumors were treated with 20 Gy once, and CSBP was administered by *i.p.* injection daily for 2 weeks (figure 5A). Compared with the negative control, CSBP treatment or local RT showed a mildly delayed tumor growth. However, the combination treatment of RT and CSBP resulted in a dramatic tumor growth regression compared with monotherapy (figure 5B). The proportion of CD8⁺ T cells and IFN- γ -expressing CD8⁺ T cells from tumor infiltrating lymphocytes (TILs) was remarkably increased after CSBP or RT treatment (figure 5C,D), and the combination of RT and CSBP treatment enhanced T-cell response. Moreover, we observed that the ratio of M1/M2 macrophages was increased by RT and/or CSBP treatment (figure 5E). Interestingly, combination of RT and/or CSBP treatment induced the local accumulation of M-MDSCs (figure 5F), consistent with the M-MDSCs phagocytosis results as described above. While, the ratio of G-MDSCs was unaffected (data were not shown). A significantly increased amount of IFN- γ -expressing CD8⁺ T cells in the draining lymph nodes and spleens of tumor-bearing mice was also observed (figure 5G,H).

CSBP combined with RT enhances antitumor activity in anti-PD-1-resistant 4T1 tumor model

The mouse mammary carcinoma 4T1 model is a well-characterized model of cold, poorly immunogenic, and anti-PD-1-resistant tumor model. In this model, we explored whether adding RT to CSBP treatment would increase antitumor immunity. The design of the

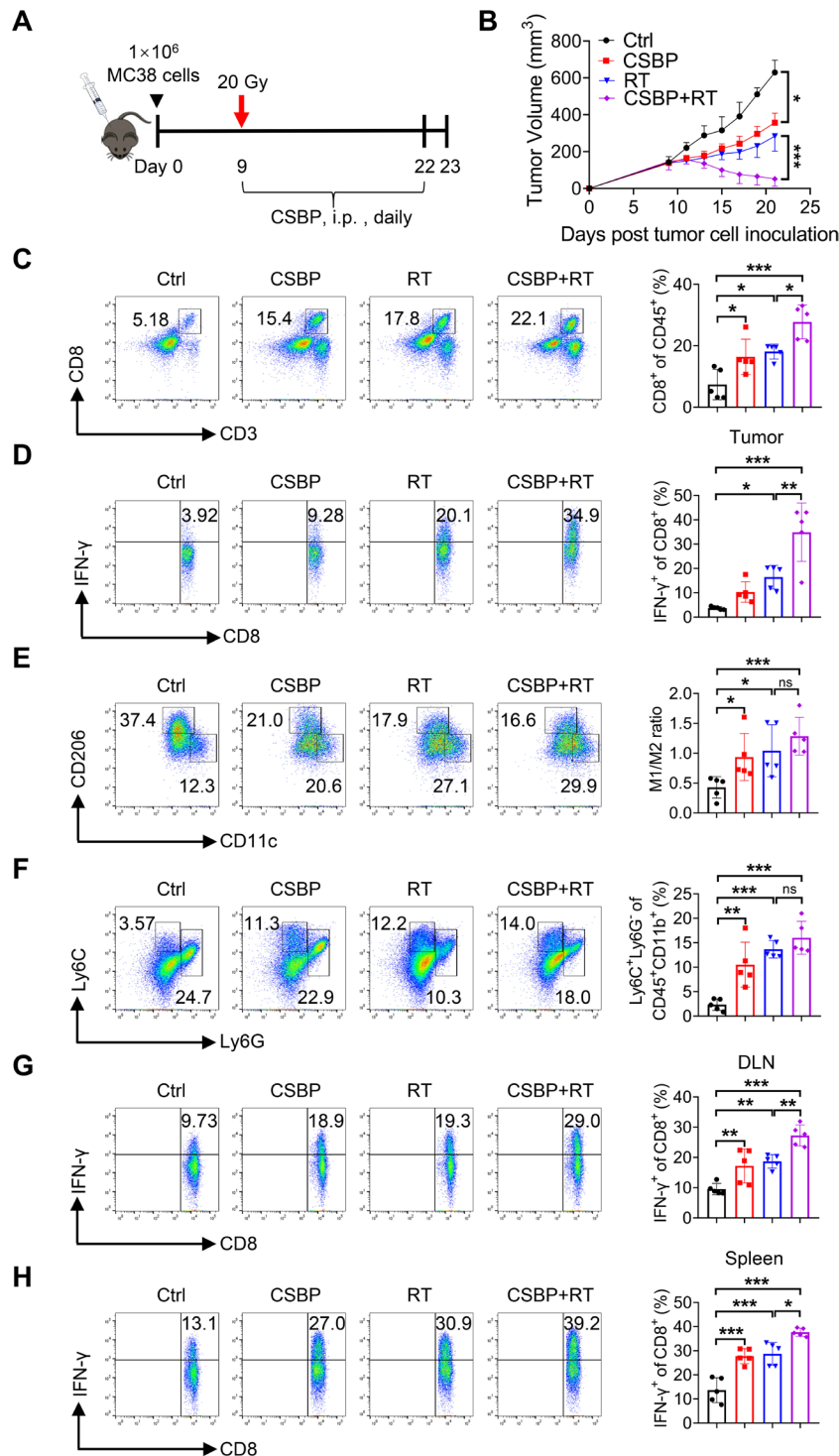


Figure 5 CSBP and RT synergistically amplify the antitumor effect in the MC38 model. (A) Schematic of the dosing schedule time points for treatment groups. (B) The tumor growth curves of MC38-bearing mice receiving the treatment of CSBP and/or RT. Data are presented as the means \pm SEM (n=5 per group). (C) The percentage of tumor-infiltrating CD8⁺ T cells in total CD45⁺ cells was determined (n=5). (D) The frequency of IFN- γ -expressing CD8⁺ T cells was detected by flow cytometry (n=5). (E) Flow cytometric analysis of M1/M2 ratio in the TME after CSBP and/or RT treatment (n=5). M1, CD45⁺ CD11b⁺ F4/80⁺ CD11c⁺ CD206⁻; M2, CD45⁺ CD11b⁺ F4/80⁺ CD206⁺ CD11c⁻. (F) Percentages of myeloid-derived suppressor cell within the TME in each group (n=5). G-MDSC, CD45⁺ CD11b⁺ Ly6G⁺ Ly6C⁻; M-MDSC, CD45⁺ CD11b⁺ Ly6G⁻ Ly6C⁺. (G, H) Cells from mice draining lymph nodes (G) or spleens (H) were obtained and stimulated with 20 ng/mL of PMA and 1 μ M ionomycin containing protein transport inhibitor cocktail for 4 hours. Frequencies of IFN- γ -expressing CD8⁺ T cells were detected by flow cytometry (n=5). Data are presented as means \pm SEM, and statistical significance was determined by two-way analysis of variance with multiple comparisons. *p<0.05, **p<0.01, ***p<0.001. CSBP, CD24/Siglec-10 blocking peptide; G-MDSC, granulocytic myeloid-derived suppressor cell; IFN, interferon; i.p., intraperitoneally; M-MDSC, monocytic myeloid-derived suppressor cell; PMA, phorbol 12-myristate 13-acetate; RT, radiotherapy; TME, tumor microenvironment.

experiment was shown in [figure 6A](#), BALB/c mice with 4T1 tumors were treated with the dosage of 12Gy for twice, and then CSBP was administrated by *i.p.* injection daily. Mice had less tumor burden with CSBP and/or RT treatment relative to the negative control ([figure 6B](#)). Similar to the results investigated above, the proportion of tumor-infiltrating CD8⁺ T cells and M-MDSCs, and the M1/M2 macrophage ratio were increased. Significantly enhanced amount of IFN- γ -expressing CD8⁺ T cells from TILs, the draining lymph nodes and spleens of tumor-bearing mice was detected ([figure 6C–H](#)). These results suggested that CSBP might have great potential to overcome PD-1 blockade resistance.

DISCUSSION

Clinical studies have demonstrated that more than 75% of patients with cancer failed to respond to ICI therapy.³¹ Moreover, PD-L1 expression level is not sufficient to be a clinical predictor, as some patients with PD-L1-expressing tumors do not respond to anti-PD-1 or anti-PD-L1 therapy, while some patients with PD-L1-negative tumors may be responsive. In this study, gene expression analysis suggested that the CD24 expression was much higher than PD-L1 in most BRCA subclasses, and single-cell RNA-sequencing data demonstrated that CD24 was expressed higher than PD-L1 in both T-cell expansion and T-cell non-expansion after anti-PD-1 treatment. The results inspired us to further investigate the potential of targeting CD24 to improve ICB response in cancer types with low-expression of the PD-L1.

Recent studies have shown that CD24/Siglec-10 delayed anti-phagocytic signals. Compared with the conventional anti-phagocytic signal CD47-Sirp α , the extensive expression of CD47 on normal tissues and cells, particularly red blood cells (RBCs), significantly increased risk of toxicity by using anti-CD47 therapeutic antibodies.⁶ Based on our data showing that CD24 is rarely expressed on normal cells and human erythrocytes, thus, CD24 can act as a therapeutic target with higher safety. Our data indicated that CD24 blockade enhanced macrophage-mediated phagocytosis of tumor cells in concordance with previous work that anti-CD24 mAb treatment enhanced phagocytic clearance of tumor cells.⁸ However, how macrophages enhance antitumor effects with CD24 blockade has not been adequately investigated in the current studies. Our results illustrated macrophages primed CD8⁺ T cells by phagocytosis of tumor cells after CSBP treatment. This role is consistent with the previous studies that macrophages as the antigen-presenting cells (APCs) that phagocytose tumor cells and present antigens to CD8⁺ T cells in response to anti-CD47 antibodies.³² CD24 and PD-L1, are considered as critical innate and adaptive checkpoints, which are extremely important for the antitumor immune response. Simultaneously targeting CD24/Siglec-10 and PD-1/PD-L1 signals is a promising strategy to reshape immunosuppressive tumor microenvironment (TME) and potentiate host innate and adaptive

antitumor immune responses. Notably, there are few studies on the simultaneous blocking of CD24 and PD-L1, and most of the CD24 or PD-L1 inhibitors are analyzed using monoclonal antibodies, which only activate macrophages or T cells. In the MC38 tumor model, compared with anti-PD-L1 monotherapy, treatment with anti-PD-L1 plus anti-CD24 as well as CSBP showed better antitumor effect, but they did not produce statistically significant effect. These results may be explained by the fact that PD-L1 is expressed on both T cells and macrophages, and anti-PD-L1 treatment enables activation of T cells and promotion of macrophage-mediated phagocytosis of tumor cells.^{33 34} The treatment of anti-PD-L1 plus anti-CD24 as well as CSBP simultaneously targeting PD-L1 and CD24 also activated T cells and enhanced macrophage phagocytosis, so the effect was not significant. Although the antitumor effect of CSBP was not as potent as anti-PD-L1, CSBP dual-targeting CD24 and PD-L1 could target tumor sites with higher specificity to exert antitumor activity. Considering that the antitumor response of CSBP might involve reshaping the TME, we examined the effect of CSBP on the immune cells of TME. As a result, CSBP substantially increased the ratios of TILs and M-MDSCs, increased the ratio of M1/M2, and enhanced the effector function of CD8⁺ T cells. By depletion of macrophages or M-MDSCs in the MC38 tumor model, the results demonstrated CSBP exerted antitumor effects partially depending on the function of macrophages and M-MDSCs.

Our study has discovered the vital coordination between tumor-cell-relation CD24 and PD-L1 for tumor evasion. It was reported that dosing RT prior to ICB could result in a systemic antitumor response.³⁵ Radiation mediates localized tumor killing and TME modification, thereby potentiating the action of ICB.³⁵ We speculated that the synergistic effects of RT combined with CSBP peptide might due to the following reasons. (1) RT can induce a local antitumor immune response by recruiting tumor-specific T cells and simultaneously increase PD-L1 expression, while the subsequent PD-1/PD-L1 blockade might amplify the antitumor response.^{30 36} CSBP can act as a PD-1/PD-L1 inhibitor, thus combining RT to CSBP treatment can boost the antitumor effectiveness. (2) RT stimulates the recruitment of macrophages to the TME. Macrophages in response to inflammatory signals produced by irradiation and are locally activated to phagocytose tumor cells.³⁷ Our results indicated that CSBP could increase the number of M1 macrophages and M1/M2 ratio. These inflammatory macrophages were used by CSBP with phagocytic capacity toward tumor cells. (3) Radiation increases the infiltration of MDSCs.³⁸ Surprisingly, it was found that M-MDSCs could also phagocytose tumor cells after CSBP treatment. Thus, RT combined with CSBP treatment is superior to monotherapy.

In addition to macrophages and CD8⁺ T cells, we found that the proportion of M-MDSC also revealed a dramatic increase following CSBP treatment or combination treatment with RT, but no significant change in G-MDSC.

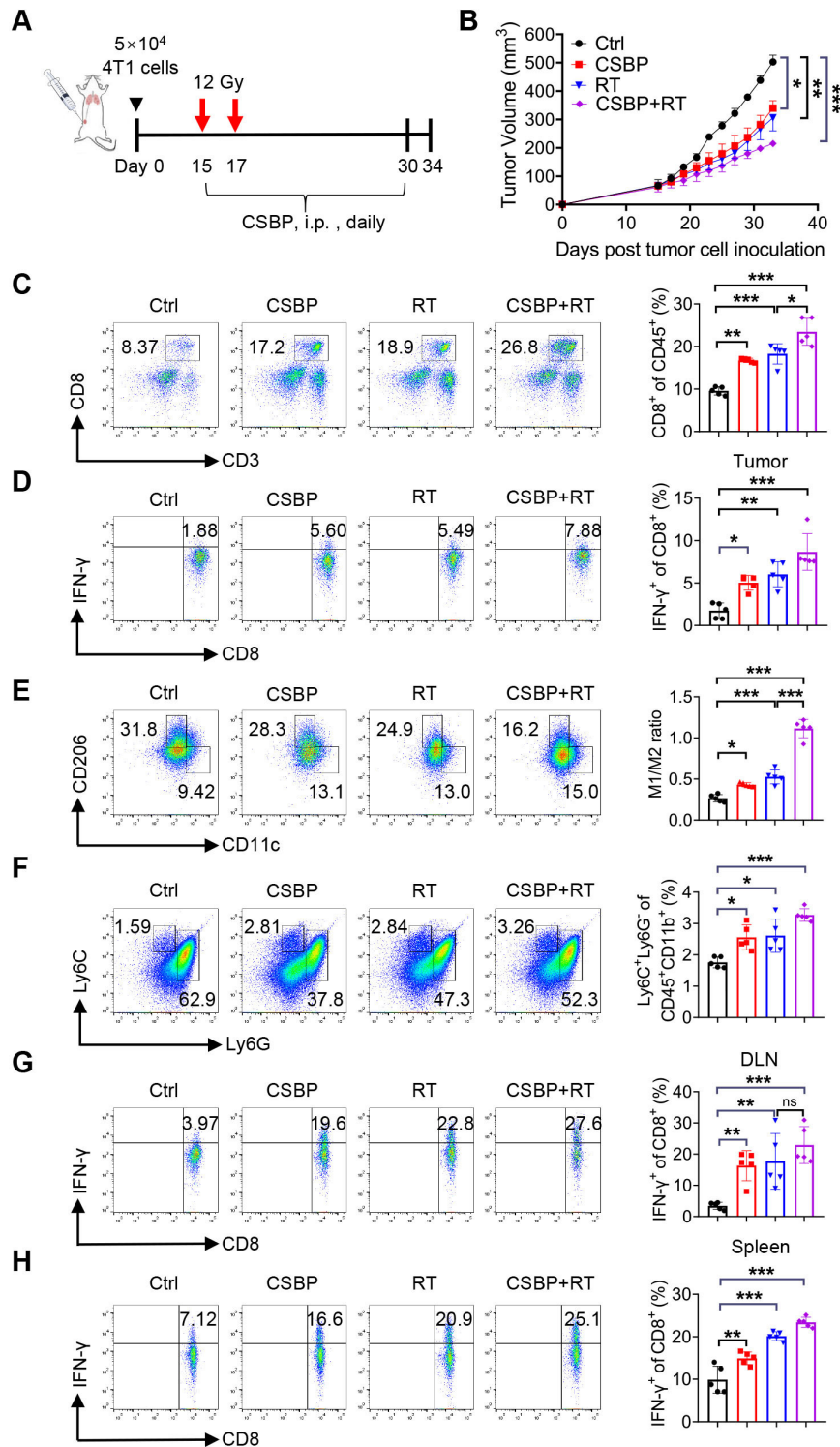


Figure 6 CSBP enhances antitumor efficacy combined with RT in the 4T1 tumor model. (A) Treatment schedules and dosing. (B) 4T1 tumor growth following CSBP and/or RT treatment in vivo. Data are presented as the means \pm SEM (n=5 per group). (C) Flow cytometric analysis of CD8⁺ T cells on CD45⁺ cells in each group (n=5). (D) The frequency of IFN- γ -expressing CD8⁺ T cells was detected by flow cytometry (n=5). (E, F) Quantitative data of the M1/M2 ratio and the percentage of myeloid-derived suppressor cells relative to CD45⁺ cells in each group (n=5). M1, CD45⁺ CD11b⁺ F4/80⁺ CD11c⁻ CD206⁻; M2, CD45⁺ CD11b⁺ F4/80⁺ CD206⁺ CD11c⁻; G-MDSC, CD45⁺ CD11b⁺ Ly6G⁺ Ly6C⁻; M-MDSC, CD45⁺ CD11b⁺ Ly6G⁻ Ly6C⁺. (G, H) Cells from mice draining lymph nodes (G) or spleens (H) were obtained and stimulated with 20 ng/mL of PMA and 1 μ M ionomycin containing protein transport inhibitor cocktail for 4 hours. Frequencies of IFN- γ -expressing CD8⁺ T cells were detected by flow cytometry (n=5). Data are presented as means \pm SEM, and statistical significance was determined by two-way analysis of variance with multiple comparisons. *p<0.05, **p<0.01, ***p<0.001. CSBP, CD24/Siglec-10 blocking peptide; G-MDSC, granulocytic myeloid-derived suppressor cell; IFN, interferon; i.p., intraperitoneally; M-MDSC, monocytic myeloid-derived suppressor cell; PMA, phorbol 12-myristate 13-acetate; RT, radiotherapy; TME, tumor microenvironment.

Previous studies found that MDSCs were a heterogeneous group of pathologically expanded myeloid cells. MDSCs suppress cytotoxic T cells and decline their antitumor activity by releasing reactive oxygen species and related cytokines.³⁹ Studies revealed that elevated MDSCs were responsible for the resistance in anti-PD-1 or anti-cytotoxic T Lymphocyte antigen 4 (CTLA-4) treatment, and elimination of MDSCs could lead to cures of metastatic tumors.⁴⁰ In this study, we found that mouse Siglec-G was overexpressed in MDSCs in mice, indicating that CD24/Siglec-10 might be a vital role of MDSC-mediated tumor cell clearance. Indeed, we observed that in vitro CD24 blockade enhanced M-MDSC-mediated phagocytosis to tumor cells, in vivo M-MDSCs were upregulated with the combination of CSBP and RT. Our work described the role for MDSCs in phagocytosis of tumor cells, and the findings differ from previous studies. However, as a heterogeneous population of myeloid cells, MDSCs possess phagocytic potential.⁴¹ A number of research studies found that G-MDSCs isolated from tumor-bearing mice could phagocytose latex beads. And previous work suggested that G-MDSCs were able to phagocytose both gram-negative and gram-positive bacteria, in common with PMN-MDSCs from tumor-bearing (cancer) dogs (C-PMNs).⁴² In fact, these are some common features between MDSCs and immature dendritic cells, such as low expression of MHC class II and antigen uptake capacity.⁴³ These results proved our hypothesis that there is a novel functional link between M-MDSCs and the efficacy of antitumor immunity. Simultaneously, we initially observed that there were no abnormalities in major organs, including heart, liver, spleen, lung and kidney, and no significant differences in red blood cell count, hemoglobin level, alanine transaminase (ALT) and aspartate transaminase (AST) levels after CSBP treatment in 4T1 and MC38 tumor models. It may require pharmacokinetics studies to further assess the in vivo safety profile of CSBP.

Taken together, our study found a CD24 and PD-L1 dual-blockade peptide, CSBP, which targeted CD24⁺ or/and PD-L1⁺ tumor cells while minimizing on-target toxicities in normal tissues. CSBP could improve cancer immunotherapy with high therapeutic efficacy by harnessing both innate and adaptive immune responses. In addition, our work described a previously uncharacterized mechanism that M-MDSC-mediated phagocytosis of tumor cells promoted potent antitumor activity. We found that CSBP and RT combination therapy exerted a synergistically antitumor effect. We believe the therapeutic approach holds promising potential to reshape the immunosuppressive tumor environment and provides new insights into the design of new therapeutics for immunotherapy.

Acknowledgements We thank all the laboratory members for helping with the experiments.

Contributors WS and YG designed the study. WS, PS, QD, and CC performed the experiments. WT, XZhu, XW, and SJ analyzed the data. XZhou, XS, YW, GC, and LQ provided advice. WS, WZ, and YG wrote and revised the manuscript. All authors read and approved the final manuscript. WZ and YG are responsible for the overall content, had access to the data and controlled the decision to publish.

Funding This work was supported by grants from the National Natural Science Foundation of China (U20A20369), Shenzhen Science and Technology Program (KQTD20190929173853397), “Pearl River Talent Plan” Innovation and Entrepreneurship Team Project of Guangdong Province (2019ZT08Y464) and Guangdong Basic and Applied Basic Research Foundation (2022B1515120085).

Competing interests None declared.

Patient consent for publication Not applicable.

Ethics approval Animal study was approved by the Ethics Committee of Sun Yat-sen University. The ethical approval number was SYSU-20200437.

Provenance and peer review Not commissioned; externally peer reviewed.

Data availability statement Data are available upon reasonable request.

Supplemental material This content has been supplied by the author(s). It has not been vetted by BMJ Publishing Group Limited (BMJ) and may not have been peer-reviewed. Any opinions or recommendations discussed are solely those of the author(s) and are not endorsed by BMJ. BMJ disclaims all liability and responsibility arising from any reliance placed on the content. Where the content includes any translated material, BMJ does not warrant the accuracy and reliability of the translations (including but not limited to local regulations, clinical guidelines, terminology, drug names and drug dosages), and is not responsible for any error and/or omissions arising from translation and adaptation or otherwise.

Open access This is an open access article distributed in accordance with the Creative Commons Attribution Non Commercial (CC BY-NC 4.0) license, which permits others to distribute, remix, adapt, build upon this work non-commercially, and license their derivative works on different terms, provided the original work is properly cited, appropriate credit is given, any changes made indicated, and the use is non-commercial. See <http://creativecommons.org/licenses/by-nc/4.0/>.

ORCID iD

Yanfeng Gao <http://orcid.org/0000-0001-5533-7100>

REFERENCES

- 1 Lesch S, Gill S. The promise and perils of Immunotherapy. *Blood Adv* 2021;5:3709–25.
- 2 Zaretsky JM, Garcia-Diaz A, Shin DS, *et al*. Mutations associated with acquired resistance to PD-1 blockade in Melanoma. *N Engl J Med* 2016;375:819–29.
- 3 Zhang S-Y, Song X-Y, Li Y, *et al*. Tumor-associated Macrophages: A promising target for a cancer Immunotherapeutic strategy. *Pharmacol Res* 2020;161:S1043-6618(20)31419-5.
- 4 Muntjewerff EM, Meesters LD, van den Bogaart G. Antigen cross-presentation by Macrophages. *Front Immunol* 2020;11:1276.
- 5 Sikic BI, Lakhani N, Patnaik A, *et al*. First-in-human, first-in-class phase I trial of the anti-Cd47 antibody Hu5F9-G4 in patients with advanced cancers. *J Clin Oncol* 2019;37:946–53.
- 6 Advani R, Flinn I, Popplewell L, *et al*. Cd47 blockade by Hu5F9-G4 and Rituximab in non-Hodgkin's lymphoma. *N Engl J Med* 2018;379:1711–21.
- 7 Wang H, Sun Y, Zhou X, *et al*. Cd47/Sirpalpha blocking peptide identification and synergistic effect with irradiation for cancer Immunotherapy. *J Immunother Cancer* 2020;8:e000905.
- 8 Barkal AA, Brewer RE, Markovic M, *et al*. Cd24 signalling through macrophage Siglec-10 is a target for cancer Immunotherapy. *Nature* 2019;572:392–6.
- 9 Hardy RR, Hayakawa K, Parks DR, *et al*. Murine B cell differentiation lineages. *J Exp Med* 1984;159:1169–88.
- 10 Crispe IN, Bevan MJ. Expression and functional significance of the J11D marker on mouse Thymocytes. *J Immunol* 1987;138:2013–8.
- 11 Williams LA, Hock BD, Hart DN. Human T lymphocytes and hematopoietic cell lines Express Cd24-associated carbohydrate Epitopes in the absence of Cd24 mRNA or protein. *Blood* 1996;88:3048–55.
- 12 Nielsen PJ, Lorenz B, Müller AM, *et al*. Altered Erythrocytes and a leaky block in B-cell development in Cd24/HSA-deficient mice. *Blood* 1997;89:1058–67.
- 13 Li O, Zheng P, Liu Y. Cd24 expression on T cells is required for optimal T cell proliferation in Lymphopenic host. *J Exp Med* 2004;200:1083–9.
- 14 Tarhriz V, Bandehpour M, Dastmalchi S, *et al*. Overview of Cd24 as a new molecular marker in ovarian cancer. *Journal Cellular Physiology* 2019;234:2134–42. 10.1002/jcp.27581 Available: <https://onlinelibrary.wiley.com/doi/10.1002/jcp.27581>

- 15 Qiao X-J, Gu Y, Du H, *et al.* Co-expression of Cd24 and Hsp70 as a Prognostic biomarker for lung cancer. *Neoplasma* 2021;68:1023–32.
- 16 Barash U, Spyrou A, Liu P, *et al.* Heparanase promotes glioma progression via enhancing Cd24 expression. *Int J Cancer* 2019;145:1596–608.
- 17 Zhou Z, Li Y, Kuang M, *et al.* The Cd24(+) cell subset promotes invasion and metastasis in human Osteosarcoma. *EBioMedicine* 2020;51:102598.
- 18 Salnikov AV, Bretz NP, Perne C, *et al.* Antibody targeting of Cd24 efficiently Retards growth and influences cytokine milieu in experimental Carcinomas. *Br J Cancer* 2013;108:1449–59.
- 19 Chan S-H, Tsai K-W, Chiu S-Y, *et al.* Identification of the novel role of Cd24 as an Oncogenesis regulator and therapeutic target for triple-negative breast cancer. *Mol Cancer Ther* 2019;18:147–61.
- 20 Conibear AC, Schmid A, Kamalov M, *et al.* Recent advances in peptide-based approaches for cancer treatment. *Curr Med Chem* 2020;27:1174–205.
- 21 Chang H-N, Liu B-Y, Qi Y-K, *et al.* Blocking of the PD-1/PD-L1 interaction by a D-peptide antagonist for cancer Immunotherapy. *Angew Chem Int Ed Engl* 2015;54:11760–4.
- 22 Zhou X, Zuo C, Li W, *et al.* A novel D-peptide identified by mirror-image Phage display blocks TIGIT/PVR for cancer Immunotherapy. *Angew Chem Int Ed Engl* 2020;59:15114–8. 10.1002/anie.202002783 Available: <https://onlinelibrary.wiley.com/toc/15213773/59/35>
- 23 Zhai W, Zhou X, Wang H, *et al.* A novel cyclic peptide targeting LAG-3 for cancer Immunotherapy by activating antigen-specific Cd8(+) T cell responses. *Acta Pharm Sin B* 2020;10:1047–60.
- 24 Bassez A, Vos H, Van Dyck L, *et al.* A single-cell map of Intratumoral changes during anti-Pd1 treatment of patients with breast cancer. *Nat Med* 2021;27:820–32.
- 25 Migoń D, Jaśkiewicz M, Neubauer D, *et al.* Alanine scanning studies of the antimicrobial peptide aurein 1.2. *Probiotics & Antimicro Prot* 2019;11:1042–54.
- 26 Lucana MC, Arruga Y, Petrachi E, *et al.* Protease-resistant peptides for targeting and intracellular delivery of Therapeutics. *Pharmaceutics* 2021;13:2065.
- 27 Yan L, Ke Y, Kan Y, *et al.* New insight into enzymatic hydrolysis of peptides with site-specific amino acid D-isomerization. *Bioorg Chem* 2020;105:S0045-2068(20)31687-4.
- 28 Shukla D, Trout BL. Understanding the synergistic effect of arginine and glutamic acid mixtures on protein solubility. *J Phys Chem B* 2011;115:11831–9.
- 29 Li W, Zhu X, Zhou X, *et al.* An orally available PD-1/PD-L1 blocking peptide OPBP-1-loaded Trimethyl Chitosan Hydrogel for cancer Immunotherapy. *J Control Release* 2021;334:376–88.
- 30 Deng L, Liang H, Burnette B, *et al.* Irradiation and anti-PD-L1 treatment synergistically promote antitumor immunity in mice. *J Clin Invest* 2014;124:687–95.
- 31 Haslam A, Prasad V. Estimation of the percentage of US patients with cancer who are eligible for and respond to Checkpoint inhibitor Immunotherapy drugs. *JAMA Netw Open* 2019;2:e192535.
- 32 Tseng D, Volkmer J-P, Willingham SB, *et al.* Anti-Cd47 antibody-mediated Phagocytosis of cancer by Macrophages primes an effective antitumor T-cell response. *Proc Natl Acad Sci U S A* 2013;110:11103–8.
- 33 Gordon SR, Maute RL, Dulken BW, *et al.* PD-1 expression by tumour-associated Macrophages inhibits Phagocytosis and tumour immunity. *Nature* 2017;545:495–9.
- 34 Hu Z, Li W, Chen S, *et al.* Design of a novel Chimeric peptide via dual blockade of Cd47/Sirpalpha and PD-1/PD-L1 for cancer Immunotherapy. *Sci China Life Sci* 2023.
- 35 Lee YH, Tai D, Yip C, *et al.* Combinational Immunotherapy for hepatocellular carcinoma: radiotherapy, immune Checkpoint blockade and beyond. *Front Immunol* 2020;11:568759.
- 36 Chen IX, Newcomer K, Pauken KE, *et al.* A bilateral tumor model identifies transcriptional programs associated with patient response to immune Checkpoint blockade. *Proc Natl Acad Sci USA* 2020;117:23684–94.
- 37 Nishiga Y, Drains AP, Baron M, *et al.* Radiotherapy in combination with Cd47 blockade elicits a macrophage-mediated Abscopal effect. *Nat Cancer* 2022;3:1351–66.
- 38 Yang X, Lu Y, Hang J, *et al.* Lactate-modulated immunosuppression of myeloid-derived Suppressor cells contributes to the Radioresistance of Pancreatic cancer. *Cancer Immunol Res* 2020;8:1440–51.
- 39 Bronte V, Brandau S, Chen S-H, *et al.* Recommendations for myeloid-derived Suppressor cell nomenclature and characterization standards. *Nat Commun* 2016;7:12150.
- 40 Kim K, Skora AD, Li Z, *et al.* Eradication of metastatic mouse cancers resistant to immune checkpoint blockade by suppression of myeloid-derived cells. *Proc Natl Acad Sci USA* 2014;111:11774–9.
- 41 Davis RJ, Silvin C, Allen CT. Avoiding Phagocytosis-related Artifact in myeloid derived Suppressor cell T-lymphocyte suppression assays. *J Immunol Methods* 2017;440:12–8.
- 42 Hlavaty SI, Chang Y-M, Orth RP, *et al.* Bacterial killing activity of Polymorphonuclear myeloid-derived Suppressor cells isolated from tumor-bearing dogs. *Front Immunol* 2019;10:2371.
- 43 Gabrilovich D. Mechanisms and functional significance of tumour-induced Dendritic-cell defects. *Nat Rev Immunol* 2004;4:941–52.